

# Deuterium astration in the local disc and beyond

Donatella Romano,<sup>1★</sup> Monica Tosi,<sup>1★</sup> Cristina Chiappini<sup>2,3★</sup>  
and Francesca Matteucci<sup>4★</sup>

<sup>1</sup>INAF – Osservatorio Astronomico di Bologna, Via Ranzani 1, I-40127 Bologna, Italy

<sup>2</sup>INAF – Osservatorio Astronomico di Trieste, Via Tiepolo 11, I-34131 Trieste, Italy

<sup>3</sup>Geneva Observatory, 1290 Sauverny, Switzerland

<sup>4</sup>Dipartimento di Astronomia, Università di Trieste, Via Tiepolo 11, I-34131 Trieste, Italy

Accepted 2006 March 7. Received 2006 March 7; in original form 2006 January 19

## ABSTRACT

Estimates of the interstellar deuterium abundance span a wide range of values. Until recently, it was customary to adopt the abundance of deuterium measured in the Local Bubble as representative of the local one. Now, it is becoming unclear whether the true local deuterium abundance is significantly higher or lower than this value, depending on the interpretation given to current data. It is important to deal with the issue of the deuterium variation and see whether it challenges our current understanding of the Galaxy evolution. To this aim, we study the evolution of deuterium in the framework of successful models for the chemical evolution of the Milky Way able to reproduce the majority of the observational constraints for the solar neighbourhood and for the Galactic disc. We show that, in the framework of our models, the lowest D/H (deuterium-to-oxygen) values observed locally cannot be explained in terms of simple astration processes occurring during the Galaxy evolution. Indeed, the combination of a mild star formation and a continuous infall of unprocessed gas required to fit all the available observational data allows only a modest variation of the deuterium abundance from its primordial value. Therefore, we suggest that depletion of deuterium on to dust grains is the most likely physical mechanism proposed so far to explain the observed dispersion in the local data.

**Key words:** ISM: abundances – Galaxy: abundances – Galaxy: evolution – cosmology: observations.

## 1 INTRODUCTION

Deuterium is created during primordial nucleosynthesis (e.g. Weinberg 1977; Boesgaard & Steigman 1985; Olive, Steigman & Walker 2000) and then destroyed in stars through  $D(p, \gamma)^3\text{He}$  reactions occurring at relatively low temperatures (of a few  $10^5$  K). Since it is hard to synthesize this loosely bound isotope in significant quantities in any astrophysical environment (Epstein, Arnett & Schramm 1976; Epstein 1977; Prodanović & Fields 2003), its abundance in galaxies is expected to monotonically decrease with time owing to stellar cycling.

Deuterium is the light nuclide produced during big bang nucleosynthesis (BBN) whose primordial abundance is most tightly tied to the baryon-to-photon ratio,  $\eta$  (or, equivalently, to the ratio of the baryon and critical densities at the present time,  $\Omega_b$ ). In principle, once its primordial abundance,  $(D/H)_p$ , is derived from measurements in unevolved systems, the value of  $\Omega_b$  is precisely known. However, there is still significant dispersion among the abundances derived for a handful of high-redshift, low-metallicity absorption-

line systems towards quasi-stellar objects (QSOs) with reasonably firm deuterium detections. A more precise  $\eta$  determination comes from the observations of the cosmic microwave background (CMB) power spectrum coupled to Ly $\alpha$  forest data (Spergel et al. 2003; see, however, Pettini 2006, his fig. 7). The suggested value,  $\eta_{10} = 6.1^{+0.3}_{-0.2}$ , where  $\eta_{10} \equiv 10^{10} \eta = 274 \Omega_b h^2$ , when coupled to predictions from the standard BBN theory, leads to a very narrow range for the primordial deuterium abundance,  $(D/H)_p \simeq 2.4\text{--}2.8 \times 10^{-5}$  (e.g. Coc et al. 2004).

Relating  $(D/H)_p$  to the current local abundance of D meets with the non-trivial issue of estimating what the *true* local abundance of deuterium actually is. In fact, a large scatter is found among nearly 50 D/H measurements towards as many Galactic lines of sight. Possible explanations (including deuterium depletion on to dust grains, or recent infall of unprocessed gas; see e.g. Prochaska, Tripp & Howk 2005; Pettini 2006, and references therein) lead to different interpretations of the data.

Up to some years ago, models for the chemical evolution of the Galactic disc were used to bound the primordial D mass fraction. Studies of this kind were motivated by the widely differing (by an order of magnitude) observational estimates of  $(D/H)_p$  published in the literature, coming from a few high-redshift QSO absorption

\*E-mail: donatella.romano@oabo.inaf.it (DR); monica.tosi@oabo.inaf.it (MT); chiappini@ts.astro.it (CC); matteucci@ts.astro.it (FM)

spectra. It was crucial then to infer  $(D/H)_p$  from the D abundance observed in the Solar system and in the interstellar medium (ISM) assuming the astration factor required to reproduce the largest set of available observational data. In general, it was found that  $(D/H)_p$  values higher than  $\sim 4\text{--}5 \times 10^{-5}$  could not be reconciled with Galactic chemical evolution (GCE) requirements (Steigman & Tosi 1992, 1995; Tosi 1996, and references therein; Tosi et al. 1998; Prantzos & Ishimaru 2001; Chiappini, Renda & Matteucci 2002), with sparse claims of the contrary (e.g. Vangioni-Flam, Olive & Prantzos 1994; Scully et al. 1997).

Recently, Kirkman et al. (2001) obtained Space Telescope Imaging Spectrograph (STIS) spectra of the Ly $\alpha$  and Lyman Limit (LL) regions of the  $z_{\text{abs}} = 0.701$  absorption system towards QSO PG 1718+4807 (the only example of a QSO absorber with a D/H ratio  $\sim 10$  times the value found towards other QSOs). They found that at least part of the extra absorption needed on the blue side of the main H I, which was previously ascribed to deuterium, is more likely due to contaminating hydrogen (see, however, Crighton et al. 2003). Even more recently, a few more low-metallicity, high-redshift QSO absorption systems have been searched for deuterium, and all show low D abundances (see the next section). This piece of evidence, together with the concordance between the  $\eta$  value obtained from the temperature anisotropies in the CMB (as well as other astronomical measurements of the power spectrum) and that suggested by the standard BBN theory for low  $(D/H)_p$  values, leads to the conclusion that  $(D/H)_p$  is indeed low, not in excess of  $3 \times 10^{-5}$  (see e.g. discussions in Romano et al. 2003; and recent reviews by Steigman 2004, 2006; Pettini 2006). At this point, it is worth mentioning that an internal tension between the abundances of the light elements created in BBN might exist – the primordial abundances of  $^4\text{He}$  and  $^7\text{Li}$  inferred from the observations being lower than those expected according to the BBN theory constrained by *Wilkinson Microwave Anisotropy Probe* (see e.g. fig. 5 of Pettini 2006). While for  $^4\text{He}$  one can appeal to previously unrecognized systematic uncertainties in the measurements (Olive & Skillman 2004), dealing with  $^7\text{Li}$  in halo stars poses awkward implications to stellar evolutionary theories. Yet, the inclusion of non-standard depletion mechanisms in stellar evolutionary models promises to reconcile the abundances observed in halo dwarfs with the primordial  $^7\text{Li}$  abundance inferred from the CMB power spectrum and the standard BBN theory (see Charbonnel & Primas 2005, for a discussion).

GCE models are, however, facing a new problem: connecting the reasonably well-known, low primordial abundance of deuterium with a presently uncertain local value. In fact, according to the newest data, the local abundance of deuterium might be either nearly

primordial, or significantly lower, quite lower than previously assumed [ $(D/H)_{\text{LISM}} = (1.50 \pm 0.10) \times 10^{-5}$ ; Linsky 1998], depending on the data interpretation.

In this paper, we will examine these new local D data in the framework of GCE models able to reproduce the vast majority of the available constraints on the disc properties. The paper is organized as follows. Measurements of deuterium at both high and low redshifts are reviewed in Section 2. The dispersion in the local data and its implications are discussed in Section 3, where the data are interpreted in the framework of complete GCE models. Finally, a discussion is presented in Section 4.

## 2 LOCAL AND HIGH-REDSHIFT DEUTERIUM DATA

Data on high-redshift, low-metallicity damped Lyman  $\alpha$  (DLA) and LL absorption systems set lower limits to the primordial abundance of deuterium. There is statistically significant scatter in the D/H measurements for about half a dozen quasar absorption systems with  $[\text{Si}/\text{H}] \lesssim -1.0$  about the mean (see Table 1). The system at  $z_{\text{abs}} = 3.025$  towards Q 0347–3819 and that at  $z_{\text{abs}} = 3.256$  towards PKS 1937–1009 are excluded from our analysis because of their complex velocity structures, which make them rather unreliable (Steigman 2004, 2006; Pettini 2006). Since the primordial D/H is thought to be isotropic and homogeneous and the metallicity of the absorption clouds used to measure D/H is low (hence no significant D astration through stars should have occurred), the scatter is hard to explain. It has been proposed that some early mechanism for D astration may be the cause for the reported scatter in D/H values (Fields et al. 2001; Prantzos & Ishimaru 2001). Yet, the correlation between D/H and  $[\text{Si}/\text{H}]$  that one would expect in this case is not seen (Fig. 1). On the other hand, unrecognized systematic effects may be responsible for an artificial dispersion in the data. In this respect, it is interesting to note that the total neutral hydrogen column density  $N(\text{H I})$  for the two systems with the highest D/H values at  $[\text{Si}/\text{H}] \lesssim -2.0$  was measured using the drop in flux at the LL. In all the other systems, the dominant constraint on the  $N(\text{H I})$  value is from the damping wings of the Ly $\alpha$  or Ly $\beta$  lines (Pettini & Bowen 2001; Crighton et al. 2004). Still, the placement of the continuum in the systems with the highest  $N(\text{H I})$  might be compromised by the presence of interlopers, and lead to erroneous  $N(\text{H I})$  determinations (Steigman 1994, 2006).

Further measurements of deuterium in metal-poor environments include that in the high-velocity, low-metallicity gas cloud Complex C falling on to the Milky Way, also listed in Table 1. Using

**Table 1.** D/H measurements towards QSOs. A weighted mean of these data (except measurements towards Q 0347–3819 and PKS 1937–1009 at  $z_{\text{abs}} = 3.256$ ; see the text for details) gives  $(D/H) = 2.6 \pm 0.3$  (the error in the mean is the dispersion about the mean divided by the square root of the number of data points), a value consistent with the primordial abundance inferred from the CMB power spectrum and the standard BBN theory.

QSO	Target <sup>a</sup>	$\log N(\text{H I})$	$z_{\text{abs}}$	$D/H \pm 1\sigma$	$[\text{Si}/\text{H}]$	$[\text{O}/\text{H}]$	Reference
PKS 1937–1009 (I)	LL	$17.86 \pm 0.02$	3.572	$(3.3 \pm 0.3) \times 10^{-5}$	$-2.7, -1.9^b$		Burles & Tytler 1998a
Q 1009+2956	LL	$17.39 \pm 0.06$	2.504	$3.98^{+0.59}_{-0.67} \times 10^{-5}$	$-2.4, -2.7^c$		Burles & Tytler 1998b
HS 0105+1619	LL	$19.422 \pm 0.009$	2.536	$(2.54 \pm 0.23) \times 10^{-5}$	$-1.85$	$-2.0$	O’Meara et al. 2001
Q 2206–199	DLA	$20.436 \pm 0.008$	2.0762	$(1.65 \pm 0.35) \times 10^{-5}$	$-2.23$		Pettini & Bowen 2001
Q 0347–3819	DLA	$20.626 \pm 0.005$	3.025	$(3.75 \pm 0.25) \times 10^{-5}$	$-0.95 \pm 0.02$		Levshakov et al. 2002
Q 1243+3047	LL	$19.76 \pm 0.04$	2.526	$2.42^{+0.35}_{-0.25} \times 10^{-5}$		$-2.79 \pm 0.05$	Kirkman et al. 2003
PKS 1937–1009 (II)	LL	$18.25 \pm 0.02$	3.256	$1.6^{+0.25}_{-0.30} \times 10^{-5}$	$-2.0 \pm 0.5$		Crighton et al. 2004
PG 1259+593	HVC	$19.95 \pm 0.05$	0.0	$(2.2 \pm 0.7) \times 10^{-5}$		$-0.79^{+0.12}_{-0.16}$	Sembach et al. 2004

<sup>a</sup>LL: Lyman limit absorption system; DLA: damped Ly $\alpha$  absorption system; HVC: high-velocity cloud.

<sup>b</sup>Blue component, red component.

<sup>c</sup>Component 2, component 3.

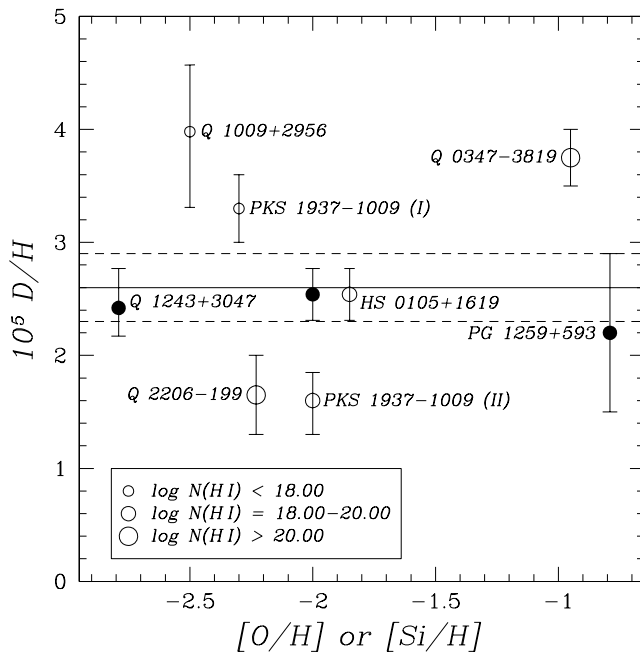


**Figure 1.** Available measurements of D/H in QSO absorption systems from Table 1. The abundance of deuterium is plotted against metallicity (either [Si/H] – open symbols, or [O/H] – filled ones). There are no hints of decreasing D/H with increasing metallicity. Rather, a large dispersion is present across the whole metallicity range. The weighted mean of the data (except for measurements towards Q 0347–3819 and PKS 1937–1009 at  $z_{\text{abs}} = 3.256$ ; see the text for details) is also shown (solid line) with its errors (dashed lines).

*Far Ultraviolet Spectroscopic Explorer (FUSE)* and *Hubble Space Telescope (HST)* observations of the QSO PG 1259+593, Sembach et al. (2004) detect D I Lyman series absorption in Complex C and derive  $(D/H)_{\text{Complex C}} = (2.2 \pm 0.7) \times 10^{-5}$ ,  $(O/H)_{\text{Complex C}} = (8.0 \pm 2.5) \times 10^{-5}$  and  $(D/O)_{\text{Complex C}} = 0.28 \pm 0.12$ . A value consistent with the primordial deuterium abundance,  $(D/H) = (2.3 \pm 0.4) \times 10^{-5}$  (weighted mean for three regions at Galactic longitudes  $l = 171^\circ, 183^\circ, 195^\circ$ ), is found also from the 327-MHz D line, for a Galactocentric distance of  $R_G = 10 \pm 1$  kpc (Rogers et al. 2005).

Precise measurements of D/H in the local interstellar medium (LISM) were obtained with *Copernicus* (e.g. Rogerson & York 1973), *HST* (e.g. Linsky 1998) and the interstellar medium absorption profile spectrograph (IMAPS; Jenkins et al. 1999; Sonneborn et al. 2000). In recent years, *FUSE* has added many determinations of D/H (as well as D/O and D/N) along several lines of sight probing the neutral ISM up to  $\sim 2.7$ -kpc away (e.g. Moos et al. 2002; Hébrard & Moos 2003; Wood et al. 2004; Hébrard et al. 2005; Oliveira et al. 2006). As data accumulated, the situation got complicated. Within the Local Bubble (LB; a low-density region within a distance of  $\sim 100$  pc in which the Sun is embedded), D/H is nearly constant. However, while Wood et al. (2004) state that  $(D/H)_{\text{LB}} = (1.56 \pm 0.04) \times 10^{-5}$ , a value derived from  $N(\text{D I})$  and  $N(\text{H I})$  measurements towards 16 targets, Hébrard & Moos (2003), who rely on measurements of D/O and O/H, find  $(D/H)_{\text{LB}} = (1.32 \pm 0.08) \times 10^{-5}$ , a value significantly lower. At  $\log N(\text{H I}) \gtrsim 20.5$  (i.e. distances greater than 500 pc), the few data points available up to now display a low deuterium abundance,  $D/H = (0.85 \pm 0.09) \times 10^{-5}$ , while in the intermediate range [ $d \sim 100$ –500 pc;  $\log N(\text{H I}) = 19.2$ –20.7] the D/H ratio is found to vary from  $\sim 0.5 \times 10^{-5}$  to  $\sim 2.2 \times 10^{-5}$  (see e.g. Linsky et al. 2005). This behaviour is interpreted as due to

deuterium depletion on to dust grains (Linsky et al. 2005; see also Prochaska et al. 2005; Oliveira et al. 2006), following an original idea by Jura (1982). According to this picture, the most representative value for the total (gas plus dust) D/H ratio within 1 kpc of the Sun would be  $(D/H)_{\text{LISM}} \geq (2.19 \pm 0.27) \times 10^{-5}$  (Linsky et al. 2005). On the other hand, on the basis of D/O and O/H measurements, Hébrard & Moos (2003) suggest that the low D/H value at ‘large’ distances truly reflects the present-epoch D/H. In their scenario,  $(D/H)_{\text{LISM}}$  should be lower than  $1 \times 10^{-5}$ .

Solar system observations of  $^3\text{He}$  permit an indirect determination of the deuterium abundance in the Protosolar Cloud (PSC; Geiss & Reeves 1972). Such an estimate of the deuterium abundance 4.5-Gyr ago,  $(D/H)_{\text{PSC}} = (2.1 \pm 0.5) \times 10^{-5}$  (Geiss & Gloeckler 1998), is remarkably similar to both the primordial and the local D/H values, if the highest D/H values measured by *FUSE* represent the actual abundance of deuterium in the vicinity of the Sun. It is worth noting that measures of deuterium in the atmosphere of Jupiter using the Galileo Probe Mass Spectrometer give a similar value,  $(D/H)_{\text{PSC}} = (2.6 \pm 0.7) \times 10^{-5}$  (Mahaffy et al. 1998).

Finally, detection of deuterium in a molecular cloud at 10 pc from the Galactic Centre indicates that  $(D/H)_{\text{GC}} = (1.7 \pm 0.3) \times 10^{-6}$  (Lubowich et al. 2000), five orders of magnitude larger than the predictions of GCE models with no continuous source of deuterium in the bulge (Matteucci, Romano & Molaro 1999). This discrepancy is suggestive of some replenishment process, likely infall of gas of cosmological composition (Audouze et al. 1976; Lubowich et al. 2000).

### 3 GALACTIC EVOLUTION OF DEUTERIUM

Once the primordial abundance of deuterium is settled thanks to (either direct or indirect) observations, the knowledge of the present-day Galactic deuterium abundance is needed to establish the degree of astration suffered by deuterium in the Milky Way. This in turn has profound implications for our understanding of the mechanisms of the formation and evolution of the Galaxy.

#### 3.1 The solar neighbourhood

If  $(D/H)_p = (2.6 \pm 0.3) \times 10^{-5}$ , and  $(D/H)_{\text{LISM}} \geq (2.19 \pm 0.27) \times 10^{-5}$  according to Linsky et al. (2005), then a low astration factor,  $f \leq 1.2 \pm 0.3$ , is required. On the other hand, if  $(D/H)_{\text{LISM}} = (0.85 \pm 0.09) \times 10^{-5}$ , as argued by Hébrard & Moos (2003), then  $f \simeq 3.1 \pm 0.7$ . Here,  $f$  is the astration factor by number

$$f = \frac{(D/H)_p}{(D/H)_{\text{LISM}}}. \quad (1)$$

In the previous work (Romano et al. 2003), we showed that the astration factor  $f \sim 1.5$  which is required in order to fulfil all the observational constraints available for the Milky Way, well reproduces also the PSC and LISM deuterium abundances, provided that  $(D/H)_{\text{LISM}} = (1.50 \pm 0.10) \times 10^{-5}$ .<sup>1</sup> Such a low astration factor is due to the combination of a moderate star formation and a continuous infall of external gas during the whole Galactic disc evolution. Noticeably, this result is almost *independent of the specific GCE*

<sup>1</sup> Often quoted in GCE works are the astration factors by mass,  $F = X_{\text{D}, p} / X_{\text{D}, t_{\text{now}}}$ , where  $X_{\text{D}, p}$  and  $X_{\text{D}, t_{\text{now}}}$  are the abundances of deuterium by mass at  $t = 0$  and  $t = t_{\text{now}} = 13.7$  Gyr, respectively.  $F$  is larger than  $f$  by a few per cent, because of hydrogen burning into helium and heavier species in the course of the Galaxy’s evolution.

*code used* (either that developed by Tosi 1988a,b; or that developed by Chiappini, Matteucci & Gratton 1997; Chiappini, Renda & Matteucci 2002). Higher astration factors ( $f \sim 2-3$ ) were suggested in the past (e.g. Galli, Palla & Ferrini 1995; Fields 1996; Prantzos 1996; but see also Chiappini et al. 1997; Tosi et al. 1998). The low one reported here is mainly due to the adoption of an updated stellar metallicity distribution, which needs more infall in order to be reproduced. Having that much infall, it comes out really hard to get larger astration factors. As stressed above, in Romano et al. (2003) we adopted the mean D/H value measured by Linsky (1998) in the LB,  $(D/H)_{LB} = (1.50 \pm 0.10) \times 10^{-5}$ , as representative of the deuterium abundance in the solar vicinity at the present time. This assumption seems now to be no longer valid in the light of recent, contrasting interpretations of the dispersion in the local data (see discussions in Section 2). Therefore, in this section we recompute the evolution of D/H.

First, we adopt various prescriptions for the stellar lifetimes and initial mass function (IMF) in a successful model for the chemical evolution of the Milky Way. Details about the model can be found in Chiappini et al. (2002) and Romano et al. (2005a), where results relevant to several chemical species are discussed. Note that here

we consider only those (IMF, stellar lifetimes) combinations which proved to guarantee a good fit to all the observational constraints available for the Milky Way (see Romano et al. 2005a). The aim is to associate a ‘theoretical error’ with our estimate of  $f$ .

In Fig. 2, we show model predictions for D/H versus [Si/H] (upper panel) and D/H versus [O/H] (lower panel) in the solar neighbourhood obtained with:

- (i) the Scalo (1986) IMF and the Maeder & Meynet (1989) stellar lifetimes (solid line);
- (ii) the Kroupa, Tout & Gilmore (1993) IMF and the Maeder & Meynet (1989) stellar lifetimes (dot-dashed line);
- (iii) the Scalo (1986) IMF and the Schaller et al. (1992) stellar lifetimes (dotted line); and
- (iv) the Kroupa et al. (1993) IMF and the Schaller et al. (1992) stellar lifetimes (dashed line).

Note that the dotted lines lay on the dashed ones, but they end up with a larger D/H at present,  $D/H = 1.9 \times 10^{-5}$  rather than  $D/H = 1.6 \times 10^{-5}$ . Indeed, different D/H and O/H ratios are reached at late times according to the different IMFs and stellar lifetimes adopted. In particular, the higher the mass of massive stars (responsible for

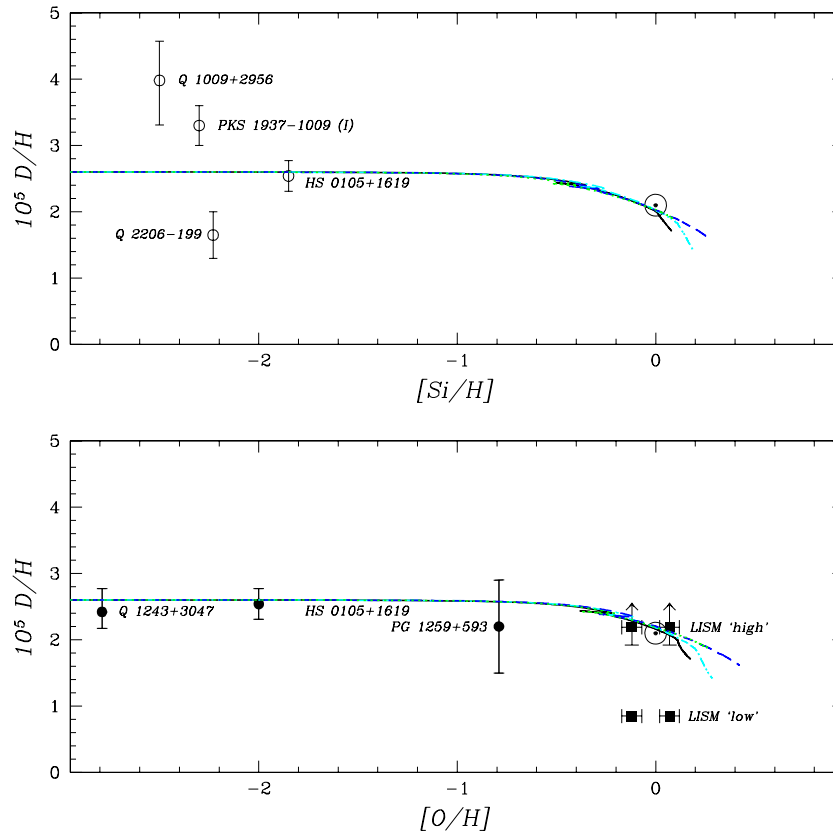


**Figure 2.** Theory versus observations. The abundance of deuterium measured in QSO absorbers (circles) is plotted against metallicity (either [Si/H] – upper panel, open circles; or [O/H] – lower panel, filled circles). Only the systems with firm D detections are considered (see Table 1 for references and Section 2 for discussion). Also shown are the deuterium abundance in the PSC (Geiss & Gloeckler 1998; upper and lower panels; Sun symbol) and those representative of the true D/H in the LISM (lower panel, squares), according to either Linsky et al. (2005; ‘high’ value) or Hébrard & Moos (2003; ‘low’ value). The values of O/H in the LISM are those measured by Oliveira et al. (2005) for the neutral ISM inside the LB,  $\log(O/H)+12 = 8.54 \pm 0.02$ , and Esteban et al. (2004) for Orion (ionized gas plus dust),  $\log(O/H)+12 = 8.73 \pm 0.03$ . Note that the Oliveira et al. measurement refers to the gas phase only, and thus misses  $\sim 25$  per cent of the total oxygen due to depletion on to dust grains. Theoretical predictions (upper panel: D/H versus [Si/H]; lower panel: D/H versus [O/H]) refer to models for the solar vicinity computed with different prescriptions about the stellar lifetimes and IMF: Scalo’s (1986) IMF and Maeder & Meynet’s (1989) stellar lifetimes (solid line); Kroupa et al.’s (1993) IMF and Maeder & Meynet’s (1989) stellar lifetimes (dot-dashed line); Scalo’s (1986) IMF and Schaller et al.’s (1992) stellar lifetimes (dotted line); Kroupa et al.’s (1993) IMF and Schaller et al.’s (1992) stellar lifetimes (dashed line). See Romano et al. (2005a), for details about the models. All ratios are normalized to the solar abundances of Asplund et al. (2005).

a quick recycling of the gas) and the lower the mass of very low mass objects (which just lock-up material, from the point of view of GCE), the lower (higher) the D/H (O/H) ratio predicted at present. The fraction of stars with initial mass  $m \geq 8 M_{\odot}$  ( $m \leq 1 M_{\odot}$ ) is larger (smaller) for the Kroupa et al. (1993) IMF than for the Scalo (1986) one (see Romano et al. 2005b, their fig. 1). This explains the different behaviours predicted by the models shown in Fig. 2. A primordial abundance of  $(D/H)_p = 2.6 \times 10^{-5}$  is assumed for all the models, i.e. the weighted mean of the most reliable QSO absorber data available in the literature (see Table 1). This value agrees well with that inferred from CMB anisotropy measurements and the standard BBN theory. Also shown in Fig. 2 are D/H measurements from QSO absorber spectra (circles; see Section 2 for references), the PSC deuterium abundance after Geiss & Gloeckler (1998; Sun symbol), and the representative  $(D/H)_{\text{LISM}}$  value according to either Linsky et al. (2005; ‘high’ value) or Hébrard & Moos (2003; ‘low’ value). Two [O/H] values are displayed for the LISM, namely that measured by Oliveira et al. (2005) for the neutral medium inside the LB,  $\log(O/H)+12 = 8.54 \pm 0.02$ , and that given by Esteban et al. (2004) for Orion,  $\log(O/H)+12 = 8.73 \pm 0.03$ , which represents the oxygen content of the ionized matter and dust. Note that part of the local oxygen is depleted on to dust grains ( $\sim 25$  per cent; see Meyer, Jura & Cardelli 1998; André et al. 2003; Cartledge et al. 2004; Oliveira et al. 2005), which brings the two measurements into agreement. All the ratios are normalized to the solar oxygen and silicon abundances from Asplund, Grevesse & Sauval (2005). An apparently striking feature of all the models is that only minor deuterium destruction is predicted as [O/H] varies on more than two orders of magnitude, increasing from  $[O/H] \leq -3$  dex up to  $[O/H] \sim -0.5$  dex. The deuterium abundance is sensibly reduced afterwards. This behaviour is easily explained by the large oxygen yield from the first Type II supernovae, which leads to a prompt oxygen enrichment of the ISM only a few million years after the onset of the star formation. Indeed, we find  $[O/H] > -3.0$  dex already 4 Myr after the onset of the star formation in the Galaxy, which raises to  $[O/H] = -0.5$  dex in the following  $\sim 300$  Myr. In the meantime, continuing infall of gas of primordial chemical composition helps to keep the D abundance near its primordial value – infall of gas is particularly strong during the early Galaxy evolution, so that the consumed D is being replenished fast by infall at those earlier times. Later on, when the contribution from low- and intermediate-mass stars (which are not net oxygen producers) to the chemical evolution of the Galaxy becomes increasingly important and the infall rate is reduced, a steeper behaviour on the D/H versus O/H plot is observed.

In Table 2, the astration factors by number for all the models displayed in Fig. 2 are listed and compared to each other. All the models well reproduce the solar abundances of oxygen and silicon at  $t = t_{\odot} = 9.2$  Gyr. A model in which the Scalo (1986) IMF and the Schaller et al. (1992) stellar lifetimes are adopted is able to destroy D at a level consistent with that suggested by Linsky et al. (2005). None of our models is able to predict astration factors larger than  $f \simeq 2$ . This leads us to favour the dust depletion scenario.

Deuterium astration in galaxies is expected to be strongly dependent on the assumptions for the two competing processes of star formation and gas infall. In Fig. 3, we compare the results obtained for D/H versus time by two GCE codes, the one of Chiappini et al. (2002; dashed line) and that by Tosi (1988a,b; solid line), once adopting the same prescriptions on the stellar lifetimes (i.e. Schaller et al. 1992) and the stellar IMF (Kroupa et al. 1993). The two models assume different prescriptions for the star formation and infall rates, yet the predicted deuterium evolution is almost the same. This

**Table 2.** Theoretical astration factors for deuterium. Listed are the astration factors by number,  $f$ , suitable for comparison with the observations. Different astration factors are predicted when assuming differing formulations for the stellar lifetimes and IMF in the GCE code.

IMF	Stellar lifetimes	Astration factors
Scalo (1986)	Maeder & Meynet (1989)	1.52
Kroupa et al. (1993)	Maeder & Meynet (1989)	1.83
Scalo (1986)	Schaller et al. (1992)	1.39
Kroupa et al. (1993)	Schaller et al. (1992)	1.61

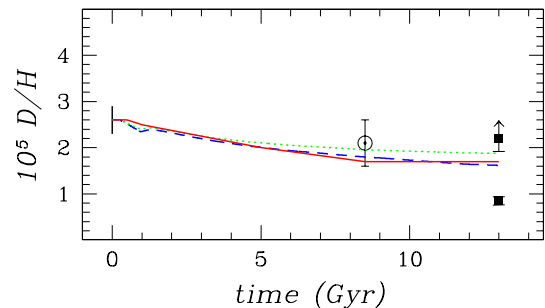


**Figure 3.** Evolution of deuterium with time in the solar neighbourhood, as predicted by two distinct codes for the chemical evolution of the Milky Way. The codes assume different star formation and infall laws, but the same IMF (Kroupa et al. 1993) and stellar lifetimes (Schaller et al. 1992 – solid and dashed lines; see the text for details). Also shown are the predictions from a code assuming Scalo’s (1986) IMF and Schaller et al.’s (1992) stellar lifetimes (dotted line). Data: vertical bar at  $t = 0$ : mean  $(D/H)_p$  from QSO absorber observations (see Section 2, for references); Sun symbol: PSC D abundance from Geiss & Gloeckler (1998); squares: fiducial ‘true’  $(D/H)_{\text{LISM}}$  value after Linsky et al. (2005; ‘high’ value) and Hébrard & Moos (2003; ‘low’ value).

is because what really matters is *the interplay* between subtraction and replenishment of gas at each time, and this interconnection is severely constrained by a number of independent observables (see e.g. Matteucci 2004). According to Fig. 3, only a mild deuterium destruction is predicted in the last 4.5 Gyr. This is consistent with the mild Galactic evolution at late times suggested by the small increase of the overall metallicity of the gas from the time of Sun formation up to now (Esteban et al. 2004, and references therein). Also the observed G- and K-dwarf metallicity distributions clearly show that the majority of the stars in the solar neighbourhood formed at low metallicities,  $[Fe/H] \leq 0$ , thus pointing again to a low star formation activity (and, hence, less evolution) at late times. Also shown in Fig. 3 is the Chiappini et al. (2002) model with Scalo’s (1986) IMF and Schaller et al.’s (1992) stellar lifetimes, which best reproduces both the solar and local ‘high’ D/H values (dotted line). It is worth emphasizing that with these prescriptions the model also well reproduces all the other observational constraints (Romano et al. 2005a).

In general, our models predict  $(D/H)_{\text{LISM}}$  values in the range  $1.4$ – $2.0 \times 10^{-5}$ . We need to enhance the ratio of the star formation to gas infall efficiencies if a larger fraction of the initial deuterium has to be destroyed. However, can a more efficient star formation and/or less effective infall of unprocessed gas be accommodated within successful GCE models? It is immediately seen that the almost constant metal abundance of the ISM from the time of Sun’s formation up to now (Esteban et al. 2004) sharply contrasts with rapid star formation and/or absence of external sources of unenriched gas. In Fig. 4, we show the outputs of a model especially designed to

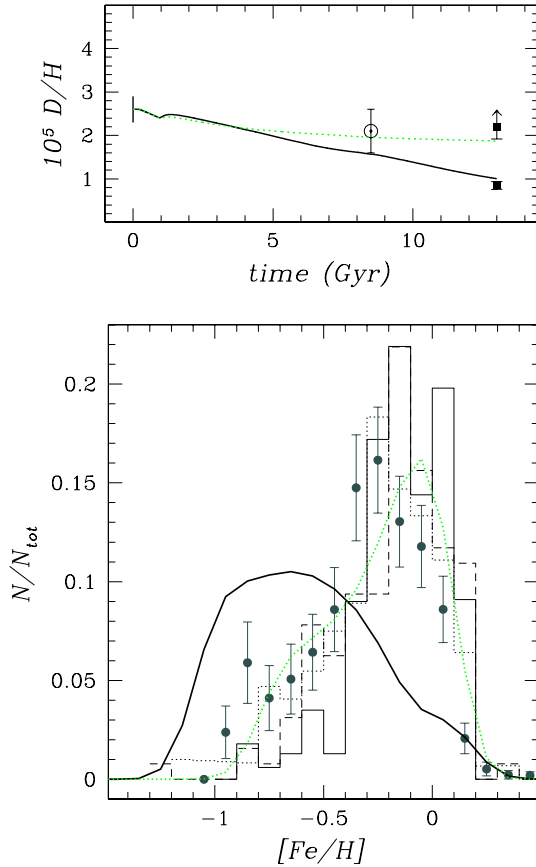


**Figure 4.** Models aimed at reproducing the lowest  $(D/H)_{LISM}$  values disagree with other important observational constraints. For instance, the model displayed in this figure (solid lines) assumes a very short time-scale for thin-disc formation in the solar neighbourhood ( $\tau_D = 1.5$  Gyr), at variance with common assumptions (see Chiappini et al. 1997). Hence, while a lower  $(D/H)_{LISM}$  can be attained (upper panel), the G-dwarf metallicity distribution of solar neighbourhood stars cannot be reproduced any more (lower panel). Also shown for comparison are the predictions of a successful model ( $\tau_D = 7$  Gyr; dotted lines), which well reproduces the shape of the observed G-dwarf metallicity distribution. This model leads to a higher  $(D/H)_{LISM}$  value. The observed G-dwarf metallicity distributions (histograms in the lower panel) are from Wyse & Gilmore (1995; dashed histogram), Rocha-Pinto & Maciel (1996; dotted histogram) and Jørgensen (2000; solid histogram). Also shown is the K-dwarf metallicity distribution by Kotoneva et al. (2002; big dots). The theoretical distributions are convolved with a Gaussian ( $\sigma = 0.1$ ) to account for the observational and intrinsic scatter.

produce a significant drop in deuterium abundance from its PSC value to the local one (for further modelling and discussions, see Tosi et al. 1998). This model, assuming  $\tau_D = 1.5$  Gyr rather than 7 Gyr for the thin-disc formation time-scale, fits the solar and local ‘low’  $D/H$  values (Fig. 4, upper panel, solid line), as well as other observational constraints (such as, for instance, the current gaseous and stellar mass surface densities at the solar position). However, it is barely consistent with the metal abundances of the Sun, it predicts a sharp increase of the metal abundance of the ISM in the last 4.5 Gyr (at variance with the observations), and it cannot account for the metallicity distribution of solar neighbourhood G- and K-dwarf stars (Fig. 4, lower panel, solid line). The metallicity distribution of long-lived stars in the solar neighbourhood is a fundamental constraint for GCE models, which mainly constrains the infall time-scale and strength (see, e.g. Chiappini et al. 1997; Matteucci

2004). In Fig. 4, lower panel, we show as a dashed, dotted and solid histogram the G-dwarf metallicity distributions observed by Wyse & Gilmore (1995), Rocha-Pinto & Maciel (1996) and Jørgensen (2000), respectively. Also shown is the K-dwarf metallicity distribution by Kotoneva et al. (2002; big dots). K dwarfs have lifetimes older than the present age of the Galactic disc, and are thus ideal stars for investigating the chemical evolution of the disc. G-dwarf stars instead are sufficiently massive that some of them have begun to evolve away from the main sequence, so that corrections must be taken into account when determining their space densities and metallicity (Kotoneva et al. 2002). These corrections are at least partly responsible for the non-negligible differences among different observational G-dwarf metallicity distributions (in particular, the low-metallicity tail of the distribution and the exact position of the peak may vary significantly according to different authors). In conclusion, in the framework of our models we cannot explain at the same time both the lowest observed  $(D/H)_{LISM}$  values and the observed G- and K-dwarf metallicity distributions.

### 3.2 Present-day abundance gradients

In Fig. 5, we display the Galactic gradients of  $D/H$ ,  $D/O$  and  $O/H$  at the present time predicted by adopting the prescriptions of Model A of Chiappini, Matteucci & Romano (2001) as far as the formation and evolution of the Galactic disc are concerned, and by varying the prescriptions for the IMF and the stellar lifetimes (solid line: Scalo’s 1986 IMF and Maeder & Meynet 1989 stellar lifetimes; dashed line: Kroupa et al.’s 1993 IMF and Maeder & Meynet 1989 stellar lifetimes; dotted line: Scalo’s 1986 IMF and Schaller et al.’s 1992 stellar lifetimes – see Romano et al. 2005a). A value of  $(D/H)_p = 2.6 \times 10^{-5}$  is assumed for all the models. Also shown are the relevant observations. The filled squares in the upper panel of Fig. 5 stand for the representative  $D/H$  value in the LISM according to either Linsky et al. (2005; ‘high’ value) or Hébrard & Moos (2003; ‘low’ value). The filled triangle in the same panel refers to the measurement by Rogers et al. (2005) for the outer Galactic disc. The filled squares in the middle panel of Fig. 5 stand for the representative  $D/O$  ratio according to either Hébrard & Moos (2003; lower value) or Linsky et al. (2005; higher value). To obtain  $(D/O)_{LISM}$  in this latter case, we divided  $(D/H)_{LISM}$  from Linsky et al. (2005) by the oxygen abundance of Orion (Esteban et al. 2004). At first glance, it seems that GCE models explain the lowest  $D/O$  value better than the highest one, while the opposite is true for  $D/H$  (upper panel). However, one should recall that the current oxygen abundance displays a non-negligible spread. Indeed, several indicators – H II regions, B-type stars and the neutral medium – show that the local oxygen abundance varies in the range  $8.3 \leq \log(O/H)+12 \leq 9.0$  (Fig. 5, lower panel, and Oliveira et al. 2006, their table 12). Therefore, in Fig. 5, middle panel, we show also the  $D/O$  ratio recently measured by Friedman et al. (2006) for the line of sight towards LSE44. Along this line of sight,  $(D/H)_{LSE44} = 2.24^{+0.70}_{-0.67} \times 10^{-5}$ , consistent with the lower limit suggested by Linsky et al. (2005), and  $(O/H)_{LSE44} = 11.3^{+4.8}_{-3.6} \times 10^{-4}$  (that is the highest  $O/H$  value measured locally by *FUSE*). Now, within the errors, the model adopting the Scalo (1986) IMF and the Schaller et al. (1992) stellar lifetimes is in satisfactory agreement with both the observed ‘high’  $(D/H)_{LISM}$  and ‘low’  $(D/O)_{LISM}$ , provided that  $(D/O)_{LISM}$  is ‘low’ as a consequence of both a high deuterium and a high oxygen abundance in the LISM.

It is seen that the shape of the gradients slightly changes when changing the prescriptions about the IMF and the stellar lifetimes. In the Galactocentric distance range  $R_G = 4\text{--}12$  kpc, the theoretical gradients of  $\log(D/H)$ ,  $\log(D/O)$  and  $\log(O/H)+12$  are



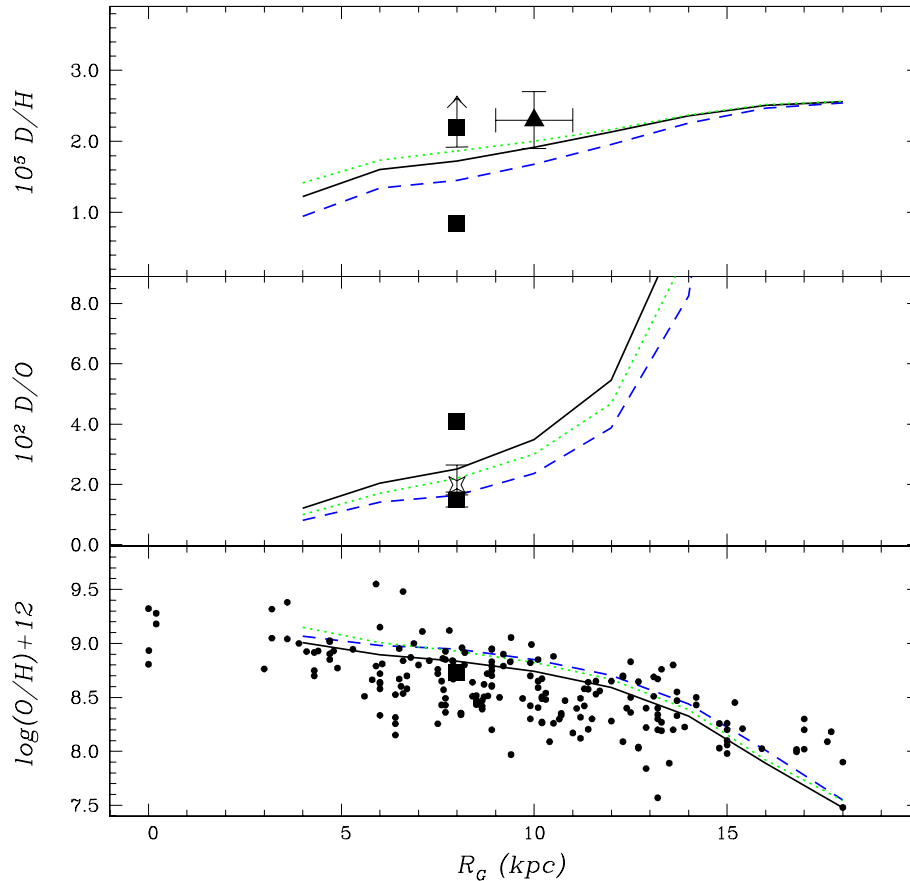


**Figure 5.** Present-day distributions of D/H (upper panel), D/O (middle panel) and  $\log(\text{O}/\text{H})+12$  (lower panel) along the disc of the Galaxy. Predictions from models assuming either the Scalo (1986) IMF and the Maeder & Meynet (1989) stellar lifetimes (solid line), or the Kroupa et al. (1993) IMF and the Maeder & Meynet (1989) stellar lifetimes (dashed line), or the Scalo (1986) IMF and the Schaller et al. (1992) stellar lifetimes (dotted line) are shown together with the relevant observations. Upper panel, filled squares: representative D/H value in the LISM according to Linsky et al. (2005; ‘high’ value) and Hébrard & Moos (2003; ‘low’ value); filled triangle: deuterium measurement from the 327-MHz D line in the outer disc (Rogers et al. 2005). Middle panel, filled squares: representative D/O value in the LISM according to Hébrard & Moos (2003; ‘low’ value) and Linsky et al. (2005; ‘high’ value) – in this case the oxygen abundance measured by Esteban et al. 2004 for Orion has been taken as representative of the total oxygen content of the LISM. Also shown (big star) is the D/O ratio towards LSE 44 measured by Friedman et al. (2006; see discussion in the text). Lower panel, small filled circles: compilation of  $\log(\text{O}/\text{H})+12$  versus  $R_G$  data from Chiappini et al. (2001); filled square: oxygen abundance in Orion from Esteban et al. (2004).

$0.03 \pm 0.01 \text{ dex kpc}^{-1}$ ,  $0.08 \text{ dex kpc}^{-1}$  and  $-0.055 \pm 0.005 \text{ dex kpc}^{-1}$ , respectively. In the outermost regions of the disc the gradient of D/H flattens, while those of D/O and O/H steepen, owing to the lower and lower amount of gas processed by stars outward in the disc.

Before concluding that, according to GCE model predictions, one shall observe D/H ratios close to the primordial value at the largest radii in spiral galaxies, it is worth reminding that the model predictions depend on a number of uncertain free parameters. Model A of Chiappini et al. (2001) produces a fairly steep O/H gradient at the largest radii (Fig. 5, bottom panel), while the majority of the data suggest a flatter behaviour. A flatter O/H gradient in the outer disc is easily obtained by suppressing the gas density threshold which regulates the star formation process during the preceding halo phase. The solid lines in Fig. 6 stand for Chiappini et al.’s (2001) Model C results. This model is analogous to Model A (Fig. 5, solid lines), except that it allows star formation in the halo to go on even when the gas density drops below the threshold value ( $\sim 4 M_{\odot} \text{ pc}^{-2}$ ). The expected D/H ratio is now  $\sim 2.5 \times 10^{-5}$  at the outermost radii, i.e. below the adopted primordial value  $[(\text{D}/\text{H})_{\text{p}} = 2.9 \times 10^{-5}$  for this

model]. Also shown in Fig. 6 are the predictions from the model of Tosi et al. (in preparation), which is an updated version of the model by Tosi (1988a,b) adopting the Kroupa et al. (1993) IMF and the Schaller et al. (1992) stellar lifetimes, and extending to the whole disc [dashed lines:  $(\text{D}/\text{H})_{\text{p}} = 2.9 \times 10^{-5}$ ; dotted lines:  $(\text{D}/\text{H})_{\text{p}} = 2.3 \times 10^{-5}$ ]. This model tends to predict higher oxygen abundances, hence lower D/O ratios, across the disc.

We conclude that, in principle, accurate measurements of both D/H and O/H in the outermost regions of spiral galaxies can allow us to discriminate among existing scenarios of galaxy formation and evolution. In fact, only minor uncertainties related to the adopted stellar yields affect the interpretation of the data in this case, owing to the well-known nucleosynthetic origin of both species. Hence, observational efforts in this direction are highly desirable.

In summary, note that all the GCE models discussed above favour minor deuterium variations [ $\Delta \log(\text{D}/\text{H})/\Delta R_G \simeq 0.02 \text{ dex kpc}^{-1}$ ] in the Galactocentric distance range sampled by current observations ( $R_G \simeq 8\text{--}11 \text{ kpc}$ ), hence favouring the highest  $(\text{D}/\text{H})_{\text{LISM}}$  determinations as representative of the local deuterium abundance.

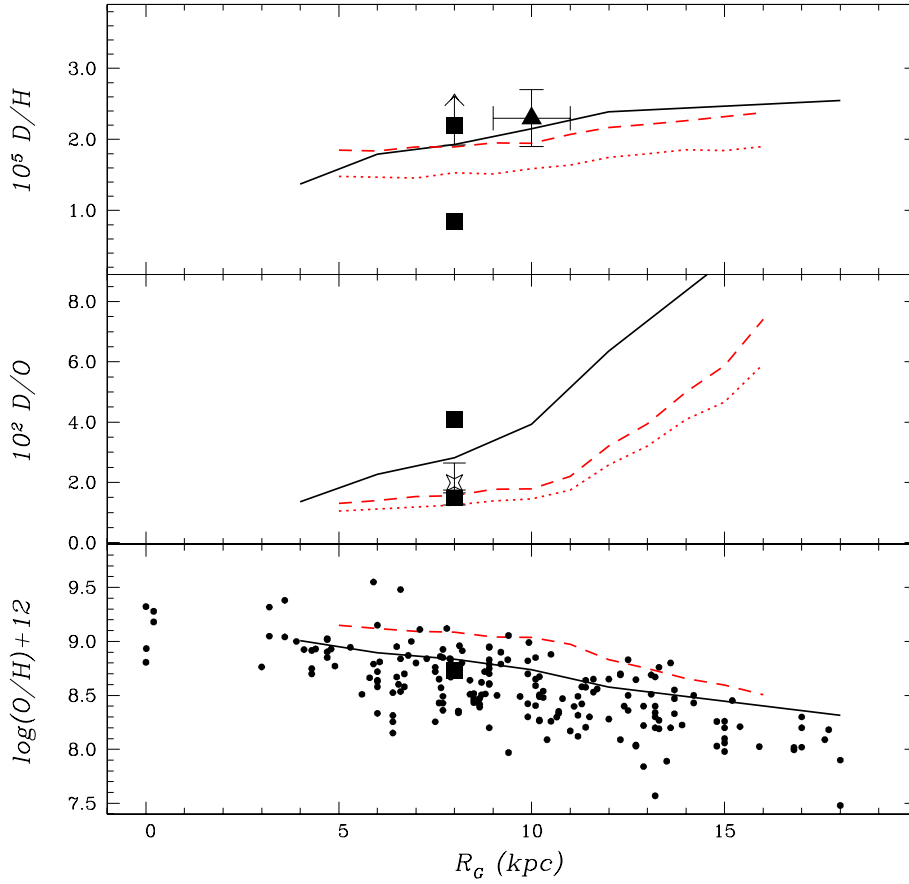


**Figure 6.** Same as Fig. 5, but for Model C of Chiappini et al. (2001; solid lines) and for the model of Tosi et al. (in preparation), which is an updated version of the model of Tosi (1988a,b) extended to the whole disc (dashed and dotted lines). Here,  $(D/H)_p = 2.9 \times 10^{-5}$  (solid and dashed lines) or  $2.3 \times 10^{-5}$  (dotted lines), and not  $2.6 \times 10^{-5}$ .

#### 4 DISCUSSION AND CONCLUSIONS

In general, observations of deuterium abundances provide *lower bounds* on its primordial abundance. However, at sufficiently high redshifts and low metallicities, one expects the primordial abundance of deuterium to reveal itself as a plateau. Instead, statistically significant scatter of the D/H measurements has been found in several high-redshift QSO absorbers. Before claiming that a dispersion around the mean value is actually present, one has to carefully check possible systematics affecting the abundance derivation. It has been suggested that in the absorbers with the lowest H I column densities, interlopers might indeed contribute to the inferred D I column densities, while in those with the highest H I column densities, interlopers might affect the wings of the H I lines (Steigman 2004, 2006, and references therein). Yet, it is worth noting that the placement of the continuum and the fitting of the damping wings are closely related for DLAs: if one gets the continuum wrong, it is unlikely that he could fit the line profile satisfactorily (M. Pettini, private communication). In this paper, we assume  $(D/H)_p = (2.6 \pm 0.3) \times 10^{-5}$ , i.e. the weighted mean of D/H measurements towards QSOs (indirect determinations give a consistent value; see discussions in Sections 1 and 2).

Of more concern is the dispersion of local D/H data. In the LISM, D/H is found to vary from  $\sim 0.5 \times 10^{-5}$  to  $\sim 2.2 \times 10^{-5}$  (Hébrard et al. 2005; Linsky et al. 2005; Williger et al. 2005; Friedman et al. 2006; Oliveira et al. 2006; to quote only the most recent works).

Basically, two mechanisms are suggested in the current literature which might explain the observed variation (Pettini 2006, and references therein; see also Lemoine et al. 1999; Prochaska et al. 2005):

- (i) differing ISM conditions along different sight lines, which determine different degrees of deuterium depletion on to dust grains;
- (ii) localized infall of unprocessed gas, which modifies the deuterium abundance in the surveyed region while leaving unchanged those of more abundant species, such as oxygen.

In the first case, one should recover the true local D/H in interstellar clouds which have been accelerated by supernova shocks, since the depletion of refractory elements is much reduced relative to that of the normal quiescent ISM there; in this case, the true local abundance of deuterium would be the highest observed one (Linsky et al. 2005, and references therein). In the second case, the true local abundance of deuterium would be the lowest observed one. In any case, the mean D/H value measured within the LB should not be considered any more as representative of the actual degree of astration suffered by deuterium in the solar neighbourhood. By assuming that the primordial abundance of deuterium is reasonably well known, one can usefully bind the deuterium astration factor of the solar vicinity. An astration factor (by number) either as low as  $f \leq 1.2 \pm 0.3$  or a factor of 2–3 higher is permitted by the observations.



In this paper, we have computed a number of GCE models for the solar vicinity as well as for the whole Galactic disc and conclude as follows.

(i) Only low astration factors (not in excess of  $f \simeq 1.8$ ) are compatible with GCE requirements: our models predict  $(D/H)_{\text{LISM}} = 1.4\text{--}2.0 \times 10^{-5}$  starting from a primordial value of  $(D/H)_p = 2.6 \times 10^{-5}$ . This is not surprising: in the absence of supernova-driven winds which efficiently remove the metal-rich ejecta of dying stars from the Galaxy and/or in the absence of a peculiar IMF, the relatively high present-day gas content and low metallicity are indicative of modest astration (and, hence, modest D destruction; see also Tosi et al. 1998). We emphasize here once again that the low astration factors are due to the combination of moderate star formation and continuous infall of gas which are needed in order to reproduce the available Milky Way data.

(ii) Small variations in the predicted D astration factor are produced by changing the prescriptions on the IMF and the stellar lifetimes. In particular, by adopting the Scalo (1986) IMF and the Schaller et al. (1992) stellar lifetimes, we predict a D astration factor which clearly favours the low one suggested by Linsky et al. (2005). With this choice for the IMF and the stellar lifetimes, the model also gives a good fit to many other observational constraints for the Galaxy (Romano et al. 2005a).

(iii) When the model is forced to reproduce the lowest D/H values observed locally, the agreement between model predictions and relevant observations is lost, for one or more observables (the most relevant observational constraints being – in this context – the G-dwarf metallicity distribution, the mild increase of the overall metallicity of the ISM from the time of Sun’s formation up to now, the present-day mass and gas surface densities, the present-day infall rate; see also Matteucci 2004).

(iv) In order to attain the lowest D/H values observed in the LISM, the smooth, gentle decline which nicely accounts for the PSC D abundance, must turn into a steeper behaviour during the latest phases of Galaxy’s evolution. However, a large gas cycling through stars in the last  $\sim 5$  Gyr is unlikely, in the light of the small increase of the global metal abundance from the time of Sun’s formation up to now suggested by several independent indicators (Esteban et al. 2004; their table 15 and references therein).

(v) In principle, joint observations of deuterium and oxygen abundances in the outermost regions of galactic discs can shed light on the mechanisms of spiral galaxy formation and evolution.

In conclusion, we favour a scenario in which D/H in the solar neighbourhood declines mildly during Galaxy’s evolution, due to the combined effect of moderate star formation and continuous infall of external gas. In this framework, the dispersion in the current local D/H data might be at least partly explained by different degrees of dust depletion along different lines of sight.

## ACKNOWLEDGMENTS

DR and MT wish to thank J. Geiss, G. Gloeckler, G. Hébrard, J. Linsky and T. Bania of the LoLa-GE Team for useful conversations at the International Space Science Institute in Bern. The warm hospitality and the financial support at ISSI are gratefully acknowledged. We are also grateful to G. Steigman for stimulating discussions and to W. Moos and M. Pettini for interesting conversations about many observational aspects. We thank J. Linsky and M. Pettini for providing us with a copy of their papers in advance of publication.

## REFERENCES

- André M. K. et al., 2003, *ApJ*, 591, 1000  
 Asplund M., Grevesse N., Sauval A. J., 2005, in Barnes T. G., III, Bash F. N., eds, *ASP Conf. Ser. Vol. 336, Cosmic Abundances as Records of Stellar Evolution and Nucleosynthesis*. Astron. Soc. Pac., San Francisco, p. 25  
 Audouze J., Lequeux J., Reeves H., Vigroux L., 1976, *ApJ*, 208, L51  
 Boesgaard A. M., Steigman G., 1985, *ARA&A*, 23, 319  
 Burles S., Tytler D., 1998a, *ApJ*, 499, 699  
 Burles S., Tytler D., 1998b, *ApJ*, 507, 732  
 Cartledge S. I. B., Lauroesch J. T., Meyer D. M., Sofia U. J., 2004, *ApJ*, 613, 1037  
 Charbonnel C., Primas F., 2005, *A&A*, 442, 961  
 Chiappini C., Matteucci F., Gratton R., 1997, *ApJ*, 477, 765  
 Chiappini C., Matteucci F., Romano D., 2001, *ApJ*, 554, 1044  
 Chiappini C., Renda A., Matteucci F., 2002, *A&A*, 395, 789  
 Coc A., Vangioni-Flam E., Descouvemont P., Adahour A., Angulo C., 2004, *ApJ*, 600, 544  
 Crighton N. H. M., Webb J. K., Carswell R. F., Lanzetta K. M., 2003, *MNRAS*, 345, 243  
 Crighton N. H. M., Webb J. K., Ortiz-Gil A., Fernández-Soto A., 2004, *MNRAS*, 355, 1042  
 Epstein R. L., 1977, *ApJ*, 212, 595  
 Epstein R. L., Arnett W. D., Schramm D. N., 1976, *ApJS*, 31, 111  
 Esteban C., Peimbert M., García-Rojas J., Ruiz M. T., Peimbert A., Rodríguez M., 2004, *MNRAS*, 355, 229  
 Fields B. D., 1996, *ApJ*, 456, 478  
 Fields B. D., Olive K. A., Silk J., Cassé M., Vangioni-Flam E., 2001, *ApJ*, 563, 653  
 Friedman S. D., Hébrard G., Tripp T. M., Chayer P., Sembach K. R., 2006, *ApJ*, 638, 847  
 Galli D., Palla F., Ferrini F., Penco U., 1995, *ApJ*, 443, 536  
 Geiss J., Gloeckler G., 1998, *Space Sci. Rev.*, 84, 239  
 Geiss J., Reeves H., 1972, *A&A*, 18, 126  
 Hébrard G., Moos H. W., 2003, *ApJ*, 599, 297  
 Hébrard G., Tripp T. M., Chayer P., Friedman S. D., Dupuis J., Sonnentrucker P., Williger G. M., Moos M. W., 2005, *ApJ*, 635, 1136  
 Jenkins E. B., Tripp T. M., Woźniak P. R., Sofia U. J., Sonneborn G., 1999, *ApJ*, 520, 182  
 Jørgensen B. R., 2000, *A&A*, 363, 947  
 Jura M., 1982, in Kondo Y., ed., *Advances in Ultraviolet Astronomy*. NASA, Washington, p. 54  
 Kirkman D. et al., 2001, *ApJ*, 559, 23  
 Kirkman D., Tytler D., Suzuki N., O’Meara J. M., Lubin D., 2003, *ApJS*, 149, 1  
 Kotoneva E., Flynn C., Chiappini C., Matteucci F., 2002, *MNRAS*, 336, 879  
 Kroupa P., Tout C. A., Gilmore G., 1993, *MNRAS*, 262, 545  
 Lemoine M. et al., 1999, *New Astron.*, 4, 231  
 Levshakov S. A., Dessauges-Zavadsky M., D’Odorico S., Molaro P., 2002, *ApJ*, 565, 696  
 Linsky J. L., 1998, *Space Sci. Rev.*, 84, 285  
 Linsky J. L. et al., 2005, *BAAS*, 37, 1444  
 Lubowich D. A., Pasachoff J. M., Balonek T. J., Millar T. J., Tremonti C., Roberts H., Galloway R. P., 2000, *Nat*, 405, 1025  
 Maeder A., Meynet G., 1989, *A&A*, 210, 155  
 Mahaffy P. R., Donahue T. M., Atreya S. K., Owen T. C., Niemann H. B., 1998, *Space Sci. Rev.*, 84, 251  
 Matteucci F., 2004, in McWilliam A., Rauch M., eds, *Carnegie Obs. Astrophys. Ser. Vol. 4, Origin and Evolution of the Elements*. Cambridge Univ. Press, Cambridge, p. 87  
 Matteucci F., Romano D., Molaro P., 1999, *A&A*, 341, 458  
 Meyer D. M., Jura M., Cardelli J. A., 1998, *ApJ*, 493, 222  
 Moos H. W. et al., 2002, *ApJS*, 140, 3  
 Olive K. A., Skillman E. D., 2004, *ApJ*, 617, 29  
 Olive K. A., Steigman G., Walker T. P., 2000, *Phys. Rep.*, 333, 389  
 Oliveira C. M., Dupuis J., Chayer P., Moos H. W., 2005, *ApJ*, 625, 232  
 Oliveira C. M., Moos H. W., Chayer P., Kruk J. W., 2006, *ApJ*, in press (astro-ph/0601114)

- O'Meara J. M., Tytler D., Kirkman D., Suzuki N., Prochaska J. X., Lubin D., Wolfe A. M., 2001, *ApJ*, 552, 718
- Pettini M., 2006, in Sonneborn G., Moos H. W., Andersson B.-G., eds, *ASP Conf. Ser. Vol. 348, Astrophysics in the Far Ultraviolet*. Astron. Soc. Pac., San Francisco, in press (astro-ph/0601428)
- Pettini M., Bowen D. V., 2001, *ApJ*, 560, 41
- Prantzos N., 1996, *A&A*, 310, 106
- Prantzos N., Ishimaru Y., 2001, *A&A*, 376, 751
- Prochaska J. X., Tripp T. M., Howk J. C., 2005, *ApJ*, 620, L39
- Prodanović T., Fields B. D., 2003, *ApJ*, 597, 48
- Rocha-Pinto H. J., Maciel W. J., 1996, *MNRAS*, 279, 447
- Rogers A. E. E., Dudevoir K. A., Carter J. C., Fanous B. J., Kratzenberg E., Bania T. M., 2005, *ApJ*, 630, L41
- Rogerson J. B., York D. G., 1973, *ApJ*, 186, L95
- Romano D., Tosi M., Matteucci F., Chiappini C., 2003, *MNRAS*, 346, 295
- Romano D., Chiappini C., Matteucci F., Tosi M., 2005a, *A&A*, 430, 491
- Romano D., Chiappini C., Matteucci F., Tosi M., 2005b, in Corbelli E., Palla F., Zinnecker H., eds, *Astrophys. Space. Sci. Library Vol. 327, The Initial Mass Function 50 Years Later*. Springer-Verlag, Dordrecht, p. 231
- Scalo J. M., 1986, *Fundam. Cosm. Phys.*, 11, 1
- Schaller G., Schaerer D., Meynet G., Maeder A., 1992, *A&AS*, 96, 269
- Scully S., Cassé M., Olive K. A., Vangioni-Flam E., 1997, *ApJ*, 476, 521
- Sembach K. R. et al., 2004, *ApJS*, 150, 387
- Sonneborn G., Tripp T. M., Ferlet R., Jenkins E. B., Sofia U. J., Vidal-Madjar A., Woźniak P. R., 2000, *ApJ*, 545, 277
- Spergel D. N. et al., 2003, *ApJS*, 148, 175
- Steigman G., 1994, *MNRAS*, 269, L53
- Steigman G., 2004, in Freedman W. L., ed., *Carnegie Obs. Astron. Ser. Vol. 2, Measuring and Modeling the Universe*. Cambridge Univ. Press, Cambridge, p. 169
- Steigman G., 2006, *Int. J. Mod. Phys. E*, 15, 1
- Steigman G., Tosi M., 1992, *ApJ*, 401, 150
- Steigman G., Tosi M., 1995, *ApJ*, 453, 173
- Tosi M., 1988a, *A&A*, 197, 33
- Tosi M., 1988b, *A&A*, 197, 47
- Tosi M., 1996, in Leitherer C., Fritze-von-Alvensleben U., Huchra J., eds, *ASP Conf. Ser. Vol. 98, From Stars to Galaxies: The Impact of Stellar Physics on Galaxy Evolution*. Astron. Soc. Pac., San Francisco, p. 299
- Tosi M., Steigman G., Matteucci F., Chiappini C., 1998, *ApJ*, 498, 226
- Vangioni-Flam E., Olive K. A., Prantzos N., 1994, *ApJ*, 427, 618
- Weinberg S., 1977, *The First Three Minutes. A Modern View of the Origin of the Universe*. Andre Deutsch, London
- Williger G. M., Oliveira C., Hébrard G., Dupuis J., Dreizler S., Moos H. W., 2005, *ApJ*, 625, 210
- Wood B. E., Linsky J. L., Hébrard G., Williger G. M., Moos H. W., Blair W. P., 2004, *ApJ*, 609, 838
- Wyse R. F. G., Gilmore G., 1995, *AJ*, 110, 2771

This paper has been typeset from a  $\text{\TeX}/\text{\LaTeX}$  file prepared by the author.